Received: 23 July 2020 | Accepted: 9 October 2020

DOI: 10.1111/gcb.15444

PRIMARY RESEARCH ARTICLE

Global Change Biology WILEY

Fungal community structure and function shifts with atmospheric nitrogen deposition

Jessica A. M. Moore[1] | Mark A. Anthony[1] | Gregory J. Pec[1] | Lidia K. Trocha[2] | Artur Trzebny[3] | Kevin M. Geyer[1] | Linda T. A. van Diepen[4] | Serita D. Frey[1]

[1]Department of Natural Resources and the Environment, University of New Hampshire, Durham, NH, USA

[2]Department of Plant Ecology and Nature Protection, Adam Mickiewicz University, Poznań, Poland

[3]Laboratory of Molecular Biology Techniques, Adam Mickiewicz University, Poznań, Poland

[4]Department of Ecosystem Science and Management, University of Wyoming, Laramie, WY, USA

Correspondence and present address
Jessica A. M. Moore, Bioscience Division, Oak Ridge National Laboratory, Oak Ridge, TN 37830, USA.
Email: mooreja1@ornl.gov

Present address
Mark A. Anthony, Department of Environmental Systems Science, ETH Zürich, Zürich, Switzerland
Gregory J. Pec, Biology Department, University of Nebraska, Kearney, NE, USA
Kevin M. Geyer, Biology Department, Young Harris College, Young Harris, GA, USA

Funding information
National Science Center of Poland, Grant/Award Number: UMO-2017/26/E/NZ8/00057; Oak Ridge National Laboratory; NSF, Grant/Award Number: DEB-1832110

Abstract

Fungal decomposition of soil organic matter depends on soil nitrogen (N) availability. This ecosystem process is being jeopardized by changes in N inputs that have resulted from a tripling of atmospheric N deposition in the last century. Soil fungi are impacted by atmospheric N deposition due to higher N availability, as soils are acidified, or as micronutrients become increasingly limiting. Fungal communities that persist with chronic N deposition may be enriched with traits that enable them to tolerate environmental stress, which may trade-off with traits enabling organic matter decomposition. We hypothesized that fungal communities would respond to N deposition by shifting community composition and functional gene abundances toward those that tolerate stress but are weak decomposers. We sampled soils at seven eastern US hardwood forests where ambient N deposition varied from 3.2 to 12.6 kg N ha^{-1} $year^{-1}$, five of which also have experimental plots where atmospheric N deposition was simulated through fertilizer application treatments (25–50 kg N ha^{-1} $year^{-1}$). Fungal community and functional responses to fertilizer varied across the ambient N deposition gradient. Fungal biomass and richness increased with simulated N deposition at sites with low ambient deposition and decreased at sites with high ambient deposition. Fungal functional genes involved in hydrolysis of organic matter increased with ambient N deposition while genes involved in oxidation of organic matter decreased. One of four genes involved in generalized abiotic stress tolerance increased with ambient N deposition. In summary, we found that the divergent response to simulated N deposition depended on ambient N deposition levels. Fungal biomass, richness, and oxidative enzyme potential were reduced by N deposition where ambient N deposition was high suggesting fungal communities were pushed beyond an environmental stress threshold. Fungal community structure and function responses to N enrichment depended on ambient N deposition at a regional scale.

KEYWORDS

atmospheric nitrogen deposition, fungi, global change, soil ecology, target-probe enrichment, temperate forest ecosystems

See also the Commentary on this article by Chen and Sinsabaugh, 27, 1322–1325.

1 | INTRODUCTION

Atmospheric nitrogen (N) deposition over the past century has increased 5- to 10-fold with industrialization in many parts of the world (Aber et al., 2003; Galloway & Cowling, 2002). Anthropogenic N inputs can eutrophy and acidify soil ecosystems, reduce native plant diversity, and suppress microbial processes (Erisman et al., 2013). Nitrogen deposition remains high in some parts of the world undergoing industrialization, and although atmospheric N deposition has declined in recent years across many parts of North America and Europe, soil communities, ecosystem productivity, and nutrient cycling continues to be impacted by historic soil N loading (Gilliam et al., 2019). Decomposition rates slow and organic matter accumulates with N deposition (Chen et al., 2018; Frey et al., 2014; Nave et al., 2009); in part, because soil fungi, key players in decomposition, are sensitive to N inputs that exceed historic loads (van Diepen et al., 2017).

Soil fungi are integral players in ecosystem carbon (Högberg & Högberg, 2002) and nutrient cycling (Burke et al., 2011; Cairney, 2012; Ekblad et al., 2013), and their response to N deposition can impact ecosystem processes. Simulated N deposition in temperate forests has reduced fungal biomass (Frey et al., 2004; Wallenstein et al., 2006; Zhang et al., 2018) and altered fungal community composition (Entwistle et al., 2013; Freedman et al., 2015; Hesse et al., 2015; Morrison et al., 2016, 2018). Shifts in soil fungal communities in response to N deposition may explain reduced rates of leaf litter (Knorr et al., 2005; Magill & Aber, 1998) and organic matter decomposition (Frey et al., 2014; Liu & Greaver, 2010; Lovett et al., 2013; Pregitzer et al., 2008; Zak et al., 2011). Decomposition slows in part due to reduced activities of extracellular enzymes, especially those associated with lignin breakdown (DeForest et al., 2004; Saiya-Cork et al., 2002; Sinsabaugh et al., 2002; Waldrop et al., 2004), which can be inferred by lower abundance of genes associated with enzyme production (Hassett et al., 2009). Richness of genes associated with breakdown of starch, cellulose, hemicellulose, and lignin declines by 12%–16% with N addition (Eisenlord et al., 2013). Chronic soil N inputs appear to promote the growth and competitive ability of N-tolerant, copiotrophic taxa, which may also have generally lower capacities for organic matter degradation (Morrison et al., 2016, 2018). This N-induced shift in the fungal community may come at the expense of taxa specializing in organic matter decomposition such as white rot fungi within the Basidiomycota (Rabinovich et al., 2004; Treseder & Lennon, 2015; Worrall et al., 1997). Precluded by a lack of data that pair fungal functional genes and community composition, it is unclear how changes in fungal community composition and function respond to N deposition at a genetic level. Relating changes in fungal community composition and biomass to functional gene composition would provide a genetic basis for conceptualizing ecosystem responses to N deposition.

Our objective was to quantify the effect of simulated N deposition on soil fungal communities and their genetic functional potential across a natural gradient of ambient N deposition (seven sites total) that vary in annual N deposition load by 3–12 kg N ha^{-1} $year^{-1}$. Five of our study sites along this gradient also included simulated long-term N deposition experiments where soils have been fertilized with 3- to 10-fold more N than ambient levels for the past 11–28 years. Previous research has primarily focused on fungal responses to experimentally simulated N deposition at individual sites (Contosta et al., 2011; DeForest et al., 2004; Eisenlord et al., 2013; Entwistle et al., 2017; Freedman et al., 2015; Frey et al., 2014; Gilliam et al., 2016; Lovett et al., 2013). We leveraged the positioning of these long-term experimental sites across a gradient of ambient N deposition to investigate fungal responses to experimental N addition in the context of varying background N deposition levels. To our knowledge, fungal responses to experimental N addition have not been investigated from the perspective of ambient N deposition, which may help to explain site-specific responses to added N. For example, a site with low background levels of N deposition may have a fungal community that would be more sensitive to eutrophication and acidification caused by experimentally elevated N inputs. Sensitivity to N inputs may be driven by community membership. Fungal community composition varies at local and regional scales (Talbot et al., 2014) and some fungal taxa decline with N deposition while others increase in abundance (Morrison et al., 2016). This differential response to N deposition is related to hyper-diverse functional profiles among fungi (Morrison et al., 2016), which vary with environmental conditions, including background N deposition levels. We hypothesized that (a) fungal biomass, richness, community composition, and functional potential would shift with experimental N addition, especially at sites with historically low ambient N deposition. Fungi at sites with low N deposition may be adapted to tolerate N limitations by producing decomposition enzymes aimed at N acquisition, but these communities may be less adapted to the environmental stress imposed by high levels of N addition (Bowman et al., 2008). We therefore further hypothesized that (b) fungal community composition would shift to having higher richness and relative abundance of those taxa known to tolerate stress; and (c) that stress tolerance functional gene relative abundance would increase while genes encoding for decomposition enzymes would decrease with experimental N additions and in association with high ambient N deposition.

We investigated microbial functional potential using a target-probe enrichment method that is novel to soil microbial ecology. Other ecological investigations of microbial functional genes have used fluorescence chip-based methods which provide information about abundance of only certain functional genes and cannot be used to examine fungi separately from bacteria in environmental (soil) samples (e.g., Zhang et al., 2017). Metagenomic approaches to characterizing soil microbial functional genes do well with bacteria and poorly with fungi because fungi have fewer rRNA gene copies than bacteria (Fierer et al., 2012). We characterized fungal functional genes using a target-probe enrichment method because it generated sequence data and can be directly related to community composition information. It was also fully customizable, enabling detection of over 20,000 functional gene variants per sample. This method

allowed us to target multiple variants of a gene that would, for example, be present in the genomes of two distantly related species. The probe enrichment method was developed for detection of DNA that is rare in the environment. It has been used to investigate ancient humans (Drosou et al., 2018; Loreille et al., 2018), Pleistocene horse species (Heintzman et al., 2017), rare and cryptic primates (Aylward et al., 2018) and wild wolf populations (Hendricks et al., 2019). Targeting specific functional genes enabled us to hone our investigation to specific fungal functions known to be important to ecosystem processes and, we hypothesized, are sensitive to N deposition.

2 | METHODS

2.1 | Site descriptions

We sampled across seven mature mixed hardwood forests, located along a natural ambient N deposition gradient spanning the east coast region of the United States (Table 1; Figure S1). Annual ambient atmospheric wet and dry N deposition ranges from 3.2 to 12.6 kg ha^{-1} $year^{-1}$ across the site gradient (National Atmospheric Deposition Program, 2016). Mean annual temperature ranges from 5 to 11°C and mean annual precipitation from 1,082 to 1,473 mm/year. The soils are Inceptisols at the five southernmost sites and Spodosols at the two northernmost sites. Dominant tree genera across sites include maple (*Acer*), beech (*Fagus*), birch (*Betula*), and oak (*Quercus*). Our sites were located between 135 and 822 m above sea level. We selected sites with as similar plant communities and abiotic factors as possible across this large geographic area by selecting sites at different elevations where tree communities and soil types were most similar (see Table 1).

Five of the seven sites had long-term simulated N deposition experiments, with fertilizer application methods varying across sites. Two experimental sites had a randomized plot design and three had paired watershed designs. At Cary Institute for Ecosystem Studies in the Catskills Mountains, NY (abbreviated NY1), 100 kg N ha^{-1} $year^{-1}$ was applied to treatment plots from 1996 to 1999, and then 50 kg N ha^{-1} $year^{-1}$ was applied from 2000 to 2006, as granular NH_4NO_3 four times per year (Lovett & Goodale, 2011). We anticipated the effects of fertilizer treatments at NY1 would be detectable in our samples because, although treatments ceased in 2006, fertilizer N applied in hardwood forests can be retained in soil for decades (Lovett & Goodale, 2011; Lovett et al., 2018). At the Soil Warming × Nitrogen Addition Study at the Harvard Forest Long Term Ecological Research site (MA), fertilization treatments began in 2006 and are ongoing. Fertilizer (50 kg N ha^{-1} $year^{-1}$) is applied at equal doses monthly to treatment plots in aqueous form during the growing season (Contosta et al., 2011). At Bear Brook Watershed in Hancock County, ME (ME), the watershed was fertilized (25 kg N ha^{-1} $year^{-1}$) bimonthly from 1989 to 2016 via helicopter by applying dry $(NH_4)_2SO_4$ (Minocha et al., 2019; Norton et al., 1999). In Bartlett Experimental Forest (NH), four 30 × 30 m plots were established with a 10 m buffer zone in 2011 and dried NH_4NO_3 is applied by hand twice during the growing season (Kang et al., 2016). Beginning in 1989 and ongoing at the Fernow Experimental Forest (watershed W3) in Fernow, WV (WV), 35 kg N ha^{-1} $year^{-1}$ is applied aerially three times per year as $(NH_4)_2SO_4$ (Gilliam et al., 2016). Two of our study sites did not experimentally manipulate N addition but represented regions with high ambient N deposition (PA and NY2, see Table 1 for site characteristics). We sampled at NY2 on June 25, 2017, at WV on June 27, 2017, at PA on June 29, 2017, at NY1 on June 30, 2017, at NH on July 6, 2017, at ME on July 7, 2017, and at MA on July 12, 2017.

2.2 | Soil collection

We collected the top 10 cm of mineral soil using a tulip bulb corer (5 cm diameter) after first removing and discarding organic horizon material. Some sites across the gradient have thin or no organic horizon; thus, we focused on mineral horizons to make cross-site comparisons. At sites with simulated N deposition treatments, we collected and homogenized into a single composite sample three soil cores within each of the four replicate control and treatment plots. At sites with ambient-only N deposition (NY2 and PA), there are no long-term plots. We therefore established four replicate sampling plots separated by at least 20 m. We collected and homogenized into a single composite sample three soil cores collected along a 1.5 m radius from the center of the plot. We chose this distance because fungal communities tend to be autocorrelated at that scale (Lilleskov et al., 2004). Soils were kept cool on ice in the field. Within 2 hr of sample collection, we subsampled and flash froze in liquid N 2 ml of soil for genomic analysis. We then sieved (<2 mm) the remaining sample, removing visible roots, rocks, and organic debris. Sieved soils were stored at 4°C prior to analysis, and flash-frozen soil subsamples for genomic analyses were stored at −20°C.

2.3 | Fungal community composition

We characterized fungal community composition by extracting DNA from subsamples (0.25 g) of frozen soil using a DNeasy PowerSoil Kit following the manufacturer's protocol (Qiagen). We quantified DNA concentration fluorometrically using a Qubit dsDNA HS kit (Invitrogen). Polymerase chain reactions (PCRs) were prepared in two technical replicates and each 5 μl reaction contained the following: 1 μl polymerase (Hot FIREPol DNA Polymerase; Solis BioDyne), 0.5 μl of each primer (2.5 μM), 2 μl ultrapure water, and 1 μl of template DNA. We used the ITS1 (TCCGTAGGTGAACCTGCGG) and ITS2 (GCTGCGTTCTTCATCGATGC) primer pair (White et al., 1990) and amplified the rRNA gene region using the thermocycler protocol as follows: 95°C by 12 min, followed by 35 cycles of 15 s at 95°C, 30 s at 50°C and 30 s at 72°C with a final extension step at 72°C for 7 min. For each sample, 3 μl of PCR was electrophoresed on a 1.5% agarose gel to check amplification efficiency. Then the

TABLE 1 Site characteristics. Sites are ordered from lowest to highest ambient N deposition. Black Rock Forest Consortium (NY2) and Kane Experimental Forest (PA) did not have simulated N deposition treatments (indicated with n/a). All other sites simulated N deposition for over 20 years. Values are means with standard deviations in parentheses for the plot-level attributes. Soil pH, C% and C:N at sites with simulated N deposition experiments are taken from control plots only

Site	Latitude, longitude	Elevation (m)	Ambient N deposition (kg ha^{-1} $year^{-1}$)	Simulated N deposition (kg ha^{-1} $year^{-1}$)	MAT (°C)	MAP (mm/year)	Soil pH	Soil C (%)	Soil C:N	Dominant trees
Cary Institute (NY1)	41.79, −73.73	136	4.4	50	8	1,082	4.3 (0.1)	23.1 (1.6)	20.0 (2.0)	*Fagus grandifolia*, *Betula lenta*, *Acer rubrum*
Bear Brook (ME)	44.87, −68.10	200	4.9	25	5	1,118	4.1 (0.4)	18.7 (7.7)	22.3 (3.1)	*Quercus rubra*, *F. grandifolia*, *Prunus serotina*
Harvard Forest (MA)	42.53, −72.18	340	7.3	50	7	1,100	3.6 (0.2)	20.0 (1.2)	20.0 (1.2)	*Q. rubra*, *Quercus prinus*, *A. rubrum*
Bartlett Experimental Forest (NH)	43.94, −71.70	332	7.7	30	7	1,270	3.9 (0.5)	5.6 (2.0)	19.7 (3.1)	*F. grandifolia*, *A. rubrum*
Fernow Experimental Forest (WV)	39.05, −79.81	823	11.4	35	9	1,473	3.5 (0.3)	17.7 (2.5)	17.7 (2.5)	*F. grandifolia*, *Betula alleghaniensis*, *Acer saccharum*
Black Rock Forest Consortium (NY2)	41.42, −74.03	214	11.5	n/a	11	1,218	3.5 (0.3)	20.0 (2.0)	23.1 (1.6)	*F. grandifolia*, *A. saccharum*, *A. rubrum*
Kane Experimental Forest (PA)	41.60, −78.77	619	11.7	n/a	7	1,100	3.7 (0.2)	14.9 (2.1)	14.9 (2.1)	*Q. rubra*, *A. rubrum*, *B. lenta*

amplicons were pooled in equimolar amounts and purified on the 2% E-Gel SizeSelect II Agarose Gels system (Invitrogen), following the manufacturer's instructions. DNA concentration and fragment length distribution of the libraries were established with the use of a High Sensitivity D1000 Screen Tape assay on a 2,200 Tape Station system (Agilent Technologies). Amplicons were sequenced using the Ion Torrent PGM system (Ion Torrent). Clonal template amplifications were performed using the Ion Torrent One Touch System II and the Ion Torrent OT2 Kit according to the manufacturer's instructions. Sequencing was carried out using the Hi-Q View Sequencing Kit and Ion 318 chip according to the manufacturer's instructions.

2.4 | Functional gene enrichment

To analyze functional gene abundance and diversity, we sequenced target fungal genes enriched using probe capture (Dowle et al., 2016). Probes were designed based on nucleotide sequences from 2,314 target genes downloaded from GenBank. We targeted three fungal genes encoding hydrolytic extracellular enzymes (*BG*, *betaglucosidase*; *CBH*, *cellobiohydrolase*; *CBD*, *cellobioside dehydrogenase*), three genes encoding oxidative extracellular enzymes (*lipH*, *lignin peroxidase*; *MNP*, *manganese peroxidase*; *LACC*, *laccase* or *laccase-like multicopper oxidase*), and four genes encoding proteins thought to confer general stress tolerance (*RHEL*, *RNA helicase*; *NTH*, *neutral trehalase*; *FKS1*, *beta-1,3-glucan synthase*; *PKS1*, *polyketide synthase*). The most abundant gene family in our target gene set was *LACC* (913 of 2,322 genes) and the second most abundant was *CBH* (700 of 2,322 genes; Table S2). A set of 20,005 probes were designed by Arbor Biosciences using proprietary algorithms seeded with the target gene sequences. Each probe was 100 nt and sequences with fewer than 100 bp were padded with Ts to reach 100 nt. The 100 nt probes were varied with 3 × tiling density, generating 34,249 candidate probes. Those probes with >94% similarity across >83% of their sequences were clustered and a single representative of each cluster was chosen for the probe set. Probe-to-probe complementarity was verified to be absent from the probe set. The custom probe set was tested by Arbor Bioscience with quality controls and standards to ensure a >97% target gene enrichment success rate. We used the MyBaits kit and followed the manufacturer's protocol to target and enrich genes in our DNA libraries.

To prepare functional gene libraries, we first sheared DNA to 350 bp segments by sonicating (Focused-ultrasonicator M220; Covaris). We prepared libraries following a PCR-free protocol (TruSeq PCR-free Prep Kit; Illumina) which included repairing fragmented ends, adenylating the 3' ends, and ligating unique index adapter sequences to the ends. We hybridized the probes with the non-pooled DNA libraries using a temperature incubation technique (Dowle et al., 2016). First, we combined 7 μl of template DNA (80–100 ng/μl) with 5 μl of an Illumina-adaptor block mixture provided in the MyBaits kit. The libraries were denatured on a thermocycler for 5 min at 95°C and 18.5 μl of a hybridization buffer was warmed for 5 min at 65°C. Then, 18 μl of each hybridization buffer was added and mixed with the DNA templates. Hybridization of probes with DNA was completed on the thermocycler for 24 hr at 65°C. MyBaits wash buffer solution was warmed to 65°C for 1 hr. DNA that hybridized with probes (i.e., probe-enriched DNA template) was isolated from non-target DNA using streptavidin-coated magnetic beads (New England Biolabs) following the manufacturer's protocol.

Bead-bound enriched templates were amplified using PCR. We eluted libraries using a 10 mM tris-TWEEN-20 solution (0.05% TWEEN, pH 8.0). Each 50 μl PCR contained 15 μl template bead-bound sample, 2.5 μl each of 10 μM forward and reverse Illumina primers (P5 and P7; Kircher et al., 2012), 25 μl of 2× Kapa HiFi HotStart ReadyMix (Kapa Biosystems), and 5 μl nuclease-free water. Amplification was completed on a thermocycler using the following program: activation at 98°C for 2 min, 16 cycles of annealing and extending (98°C for 20 s, 60°C for 30 s, 72°C for 40 s), a final extension at 72°C for 5 min, and infinite hold at 8°C. Amplified enriched libraries were checked visually on an electrophoresis gel and purified for sequencing (AxyPrep Mag; Axygen). The purified library concentrations were quantified fluorimetrically (Qubit; Invitrogen) and pooled at equimolar concentrations. Sequencing was performed on an Illumina Next-Seq 150 platform at the Center for Genomics and Bioinformatics (CGB) at Indiana University (Bloomington, Indiana, USA).

2.5 | Bioinformatics

Fungal community composition was characterized by first pre-filtering raw sequence data by Ion Torrent Suite software version 5.10.1 (Life Technologies) to remove polyclonal and low-quality sequences. Sequence reads shorter than150 bp were removed from the dataset. Leading and trailing low-quality or unknown/unidentified nucleotides were removed using Trimmomatic ver. 0.39 (Bolger et al., 2014). Fastx toolkit (Hannon, 2010) was used to extract sequences with the minimum of 50% of bases with a quality score ≥25. Quality-filtered sequences were separated into individual combinations of indexes in Geneious R11.1.5 (https://www.geneious.com). Next, the sequences were trimmed at 5′ and 3′ ends to exclude PCR primers. The USEARCH (v11; Edgar, 2010) pipeline was then used to create an operational taxonomic unit (OTU) table. Quality control sequences (5 million) were dereplicated and singletons were removed (453, 976) using the -fastx_uniques and -sortbysize algorithms. We then removed chimeras (1,664) and clustered sequences at 97% similarity using the -cluster_otus algorithm. A total of 5,083 OTUs were clustered. We then used Sintax to predict the taxonomy of OTUs using the utax reference dataset and the -makeudb_usearch and -sintax functions (Edgar, 2016). None of the sequences were assigned to non-fungal organisms, 88% and 49% of the OTUs were assigned taxonomy at the phylum and genus levels, respectively. Genus-level assignments were used to predict the functional guild of taxa using FUNGuild (Nguyen et al., 2016), and all "probable" or higher-level designations were included, with 46% of the OTUs assigned a functional guild.

The OTU table was rarefied to the lowest sequencing depth (642 sequences per sample) using the *rarefy* function in vegan (Oksanen et al., 2013). We then used the *diversity* function in vegan with the "index" parameter set to "Shannon" to calculate the Shannon–Weaver alpha diversity and approximate fungal richness. The relative abundance of OTUs was then converted to a Bray–Curtis dissimilarity matrix using the *vegdist* function. We tested the effects of N addition, ambient N deposition level, and their interaction on fungal community composition using the *adonis* function after 999 permutations. Functional gene abundances and biogeochemical covariates were correlated to community composition using the *vegdist* function after 999 permutations. Variation in fungal community composition was visualized using non-metric multidimensional scaling and the metaMDS function. Finally, we performed indicator species analysis to determine whether taxa were exclusively found in certain treatment groups and if these taxa were commonly found in certain treatment groups, as revealed by the A and B components of indicator species analysis, respectively. Indicator species analysis was performed using the *multipatt* function within the indicspecis package (De Caceres & Legendre, 2009).

To analyze functional gene composition, we created a reference sequence database based on the 20,005 probes. We constructed a reference file using the Burrows–Wheeler Aligner's Smith–Waterman alignment (Li & Durbin, 2010) using the "index" function implemented in Qiime v1.9 (Caporaso et al., 2010). Illumina HiSeq data were initially demultiplexed and quality filtered at the CGB at Indiana University (Bloomington, Indiana, USA). Primer sequences, sequences <100 bp, and bases with minimum quality scores of <25 were removed by CGB using Trimmomatic. All remaining forward and reverse reads were merged allowing a 15% mismatch rate and default parameters for the method *join_paired_ends.py* in Qiime v1.9. Only paired sequences ≥100 bp were retained using the *sortbylength* command in USEARCH v9.2 (Edgar, 2010). QC sequences were then mapped to our indexed reference file using *map_reads_to_reference.py* in Qiime v1.9 using default parameters.

We quantified the relative abundance and composition of 10 protein-encoding sequences (*BG*, *CBD*, *CBH*, *FKS1*, *LACC*, *lipH*, *MNP*, *NTH*, *PKS1*, and *RHEL*). Unique functional gene OTUs that did not map to the reference were identified using the BLASTn program (Benson et al., 2005). We calculated relative abundance of each target gene in each of the 48 soil samples. We grouped them based on ecological significance: hydrolytic enzymes, oxidative enzymes, and stress tolerance.

2.6 | Soil biogeochemistry

We measured biogeochemical and edaphic parameters important to fungal physiology and community structure, including soil moisture content, pH, texture, total soil C and N, C and N mineralization, and fungal biomass. Soil moisture content was measured gravimetrically by drying samples for at least 48 hr at 105°C. Soil pH was determined in distilled water at a 1:2 (w/v) ratio using potentiometry. Soil texture was assessed on 30 g of field-moist soil using the hydrometer method (Robertson et al., 1999). Soil C and N content was measured on air-dried and finely ground subsamples (10 g) using an elemental analyzer (Perkin Elmer 2400 Series II CHN). To estimate C and N mineralization, we incubated 20 g field-moist soil for 28 days in the dark at 25°C in sealed Mason jars. We collected 2 ml headspace gas samples each day for the first seven days and on days 14 and 28. Anaerobic activity was minimized by flushing the jars with CO_2-free air after each sampling. Carbon efflux was measured on an infrared gas analyzer (LiCor 7500). We extracted inorganic N using 2 M KCl (40 ml) from soil subsamples (10 g) taken prior to and after the incubation. Inorganic N was determined as the sum of NH_4^+ and NO_3^- measured colorimetrically (Braman & Hendrix, 1989), and N mineralization rate was calculated as the difference between final and initial total soil inorganic N concentrations. Microbial biomass C and N were calculated as the difference between C and N concentrations in samples that were not fumigated with chloroform and those that were fumigated for 24 hr in the dark at room temperature (Vance et al., 1987).

Fungal biomass was estimated using phospholipid fatty acid (PLFA) analysis on freeze-dried soil samples (Guckert et al., 1985; White et al., 1979). Lipids were extracted from freeze-dried soil (1 g) using phosphate buffer, chloroform, and methanol (0.8:1:2 v:v:v). The polar lipids were isolated and purified using silicic acid chromatography and methanol. Polar lipids were then methylated in 0.2 M methanolic potassium hydroxide (1 ml) at 60°C for 30 min to form fatty acid methyl esters (FAMES). FAMES were dried and reconstituted in hexane for quantification on a Varian CP-3800 gas chromatograph equipped with a flame ionization detector. We compared FAME peaks against a standard library of FAMES specific to fungi (18:2w6,9c, 18:1w9c; Matreya). Standard biomarkers were used to convert peak area concentrations into nmol PLFA per g dry soil.

2.7 | Statistics

We analyzed the effect size of fungal responses to simulated N deposition treatments across the gradient of ambient N deposition. The effect size of fungal biomass, fungal richness, and functional gene relative abundance responses to simulated N deposition were calculated as the log response ratio for each site (LRR_{Site}) as follows:

$$LRR_{Site} = \ln(\bar{Y}_N) - \ln(\bar{Y}_C),$$

where $\bar{Y}_N$ and $\bar{Y}_C$ are mean values for the fertilized and control treatments, respectively. We tested the fit of a random effects model to our data using the package metafor in R (Viechtbauer, 2010). We calculated LRRs and variance by specifying the ROM method in the *escalc* function and estimated model fit by specifying the restricted maximum-likelihood estimator method in the *rma* function (Viechtbauer, 2005). Annual N deposition rate reported for 2016 (National Atmospheric Deposition Program, 2016) was included as a fixed effect. We interpreted a response as increasing with fertilizer treatments relative to

control if LRR_{Site} was greater than 1. If the confidence interval for LRR encompassed 1, we interpreted that as no effect of simulated N deposition on the response variable and we report the omnibus test statistic Q_M. Effect sizes for fungal biomass, oxidative enzyme encoding gene relative abundance, hydrolytic enzyme encoding gene relative abundance, and stress-response protein encoding gene relative abundance were regressed against ambient N deposition, soil C percent, soil C:N, soil clay percent, and site elevation in univariate models. We calculated the Akaike information criterion adjusted for small sample size (AICc) using the package MuMIn (Bartoń, 2020) in R; models within two AICc points of each other were considered statistically similar and the lowest AICc score was considered the best-fit model. We analyzed the correlation between ambient N deposition and the relative abundance of each of the 10 target genes and report Pearson's correlation coefficient (r).

3 | RESULTS

Climate and vegetation characteristics were relatively constant across the ambient N deposition gradient, but soil biogeochemical patterns markedly varied. Soil pH ranged from 3 to 5 and declined with increasing ambient N deposition ($p < .001$, $R^2 = .35$; Figure S2a). Soil pH was not affected by N fertilization when considering all sites together ($p = .43$, $\chi^2 = 0.64$) or in association with particular ambient N deposition levels ($p = .74$, $Q_M = 0.11$). Soil C:N ranged from 12.9 to 25.6 and declined with ambient N deposition ($p = .03$, $R^2 = .14$; Figure S2b). Soil C:N was not different between fertilized and control plots ($p = .63$, $\chi^2 = 0.23$); C:N responded to fertilizer treatment differently across sites such that it increased with fertilizer more under high ambient N deposition than low ($p = .05$, $Q_M = 3.72$). Microbial biomass C and N declined ($p = .02$, $R^2 = .09$; $p < .001$, $R^2 = .29$) with ambient N deposition. Total microbial biomass was similar in fertilized and control plots ($p = .32$, $\chi^2 = 0.98$), and this effect was consistent across the gradient ($p = .11$, $Q_M = 7.6$). Rates of C mineralization were not different in fertilized and control plots ($p = .74$, $\chi^2 = 0.11$), and this response did not change across the gradient ($p = .25$, $Q_M = 1.33$). In summary, most biogeochemical parameters varied across the ambient N deposition gradient but were unaffected by N fertilization, except soil C:N which responded to fertilizer treatments differentially across the gradient of ambient N deposition.

3.1 | Variation in fungal communities and soil biogeochemistry across the ambient N deposition gradient

Total fungal biomass did not vary across the ambient N deposition gradient ($p = .84$), but community composition was significantly different across sites ($p = .001$, $F = 1.7$; Figure 1; Table 2). Fungal community composition was significantly associated with N mineralization ($p = .005$, $R^2 = .35$; Figure 1; Table 3), the relative abundance of fungal decomposition

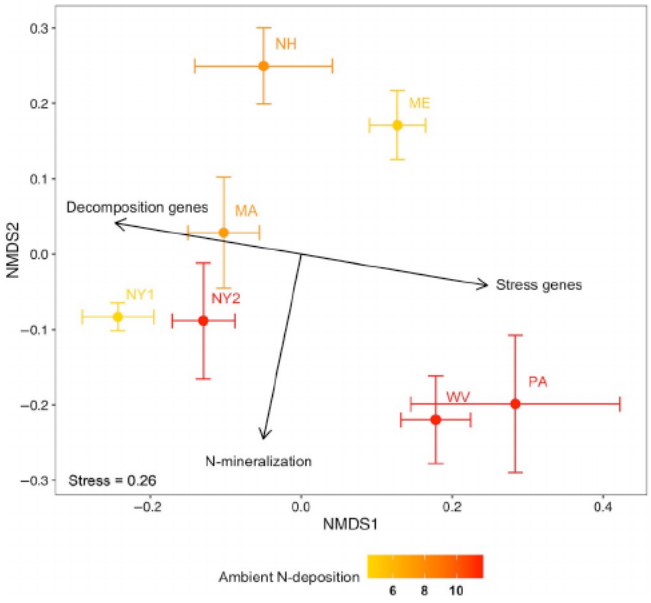

FIGURE 1 Fungal operational taxonomic unit composition in control plots at each site across the ambient N deposition gradient. Each point represents average composition and bars represent standard error. The color gradient indicates ambient N deposition level going from low (yellow) to high (red). Vectors show significant correlation between fungal community composition and N mineralization and the relative abundances of decomposition and stress tolerance functional genes (see Table 3 for correlation statistics)

TABLE 2 PERMANOVA model output showing impacts of ambient N deposition and simulated on fungal community composition

	R^2	F	p
Ambient N deposition	**.04**	**1.7**	**.001**
Simulated N deposition	.01	0.78	.99
Simulated × Ambient	.02	0.97	.62

Bold values indicate significance at $p < .05$.

TABLE 3 Pearson's correlations between fungal community composition (Bray–Curtis dissimilarity) and environmental variables or functional gene relative abundances

Variable	R^2	p
Latitude	.02	.77
Soil pH	.11	.09
C:N ratio	.11	.11
N mineralization	**.35**	**.005**
C mineralization	.02	.62
Decomposition genes	**.25**	**.008**
Stress genes	**.25**	**.008**
Oxidative genes	.08	.24
Hydrolytic genes	.02	.70

Bold values indicate significance at $p < .05$.

TABLE 4 Indicator species analysis for control soils at each site along the ambient N deposition gradient. Sites are ordered from lowest to highest ambient N deposition (refer to Table 1). Fungal taxa that are significant indicators of community composition at each site are shown (top five taxa). The A component indicates how exclusive the taxon was to a site where a value of 1 indicates the OTU was exclusively found at that site. The B component indicates how frequently that taxon was found in replicate soil samples within sites, where 1 means it was found in every sample. The indicator value accounts for both the A and B components together

Site	A component	B component	Indicator value	Taxonomy	Ecology
NY1	1	0.75	0.87	*Russula* sp. 54	Ectomycorrhizal
	1	0.623	0.79	*Cenococcum geophilum* 119	Ectomycorrhizal
	1	0.63	0.79	*Elaphomyces* sp. 636	Ectomycorrhizal
	0.97	0.63	0.78	*Cortinarius* sp. 48	Ectomycorrhizal
	1	0.5	0.71	*Russula aeruginea* 31	Ectomycorrhizal
ME	1	0.38	0.61	*Sebacina* sp. 26	Ectomycorrhizal
	1	0.38	0.61	*Sebacina* sp. 277	Ectomycorrhizal
	1	0.38	0.61	*Tomentella* sp. 113	Ectomycorrhizal
	1	0.38	0.61	*Clavulina castaneipes* 155	Ectomycorrhizal
	1	0.38	0.61	*Helotiales* sp. 384	Unknown
MA	1	0.57	0.76	*Russula variata* 4,466	Ectomycorrhizal
	0.97	0.57	0.74	*R. variata* 94	Ectomycorrhizal
	1	0.43	0.66	*Hyaloscyphaceae* sp. 767	Saprotroph
	1	0.43	0.66	*Blastocladiomycetes* sp. 1,210	Unknown
	0.88	0.43	0.61	*Thelephoraceae* sp. 135	Ectomycorrhizal/ Saprotroph
NH	1	0.38	0.61	*Clavariaceae* sp. 71	Unknown
	1	0.38	0.61	*Clavulinopsis fusiformis* 502	Saprotroph
	1	0.38	0.61	*Sebacina* sp. 590	Ectomycorrhizal
WV	1	0.5	0.71	*Leohumicola* sp. 874	Saprotroph/ Endophyte
	0.95	0.5	0.69	*Inocybe* sp. 398	Ectomycorrhizal
	1	0.38	0.61	*Clavariaceae* sp. 16	Unknown
	1	0.38	0.61	*Hygrocybe chlorophana* 126	Saprotroph/ Endophyte
	1	0.38	0.61	*Archaeorhizomyces* sp. 256	Saprotroph
NY2	0.96	0.75	0.85	*Cuphophyllus lacmus* 35	Saprotroph/ Endophyte
	0.71	0.75	0.73	*Russula silvestris* 133	Ectomycorrhizal
	0.7	0.75	0.73	*Umbelopsis dimorpha* 43	Saprotroph
	1	0.5	0.71	*Boletus* sp. 99	Ectomycorrhizal
	1	0.5	0.71	*Russula* sp. 177	Ectomycorrhizal
PA	1	0.75	0.87	*Xylonomycetes* sp. 461	Unknown
	1	0.5	0.71	*Archaeorhizomycetes* sp. 148	Saprotroph
	1	0.5	0.71	*Archaeorhizomyces* sp. 363	Saprotroph
	1	0.5	0.71	*Mortierella alliacea* 390	Saprotroph
	1	0.5	0.71	*Xylonomycetes* sp. 435	Unknown

encoding genes ($p = .008$, $R^2 = .25$; Figure 1; Table 3) and stress tolerance encoding genes ($p = .008$, $R^2 = .25$; Figure 1; Table 3). Sites with the highest ambient N deposition levels had community compositions that were associated with higher relative abundance of stress tolerance encoding genes while communities where ambient N deposition was lowest were associated with higher relative abundance of decomposition encoding genes. Shannon index declined ($p = .004$, $R^2 = .15$), but taxonomic richness did not vary with ambient N deposition ($p = .52$).

Taxa that were indicative of fungal community composition were ectomycorrhizal (ECM) where N deposition was low and primarily saprotrophic where N deposition was high (Table 4). Several fungal indicator taxa were exclusively found at sites on opposite ends of the ambient N deposition gradient (Figure 2; Table 4). Indicator ECM taxa found exclusively at sites with low ambient N deposition (4–4.9 kg N ha^{-1} $year^{-1}$) included species of *Russula*, *Cenococcum*, *Elaphomyces*, *Cortinarius*, and *Sebacina*. Saprotrophic indicator taxa, along with a few other ECM, were exclusively found in plots with >11 kg N ha^{-1} $year^{-1}$, including saprotrophic *Cladophialophora*, *Leohumicola*, *Hygrocybe chlorophana*, *Archaeorhizomyces* sp., *Mortierella alliacea*, and *Serpula himantioides*. Relative abundance of ECM declined with ambient N deposition in the control plots across the gradient ($p = .04$, $R^2 = .16$; Figure 2a) and saprotrophs did not vary ($p = .15$, $R^2 = .06$; Figure 2a). The ratio of ECM to saprotrophic fungal relative abundance also did not vary across the gradient ($p = .16$, $R^2 = .06$; Figure 2a).

Functional gene composition and relative abundances in control plots shifted across the ambient N deposition gradient (Figures 3 and 6). The composition of the 20,000 functional gene variants significantly varied with ambient N deposition ($p = .001$, $R^2 = .16$) and soil C:N ($p = .001$, $R^2 = .17$). Each functional gene group contained tens to thousands of different gene variants. At the functional group level, we found that relative abundances of the groups responded differently to ambient N deposition (Figure 4). The relative abundance of genes encoding hydrolytic enzymes were either neutral or positively correlated with ambient N deposition (*BG*, $p = .15$, $R^2 = .04$; *CBH*, $p = .11$, $R^2 = .05$; *CBD*, $p = .001$, $R^2 = .46$). Oxidative enzyme encoding gene relative abundances were all significantly negatively correlated with ambient N deposition (*LACC*, $p = .02$, $R^2 = .15$; *lipH*, $p = .01$, $R^2 = .16$; *MNP*, $p = .002$, $R^2 = .26$). One gene encoding a protein involved in stress tolerance had relative abundance that was positively correlated with ambient N deposition (*RHEL*, $p = .001$, $R^2 = .37$) and the other three stress tolerance protein-encoding genes were not correlated with ambient N deposition ($p > .05$).

3.2 | Effect of N fertilizer treatments across the ambient N deposition gradient

While fungal biomass ($p = .81$, $\chi^2 = 0.06$) and community structure did not vary with N fertilizer additions overall (Table 2), the effect of fertilizer treatments on these parameters varied across the gradient. Fungal biomass increased with fertilizer additions where ambient N deposition was low, while it decreased where ambient N deposition was high ($p = .005$, $Q_M = 7.81$; Figure 5a). Fungal biomass increased with fertilizer treatments at low elevations and decreased with fertilizer treatments at high elevation (Table S2). Likewise, the response of OTU richness to fertilizer addition varied across the N deposition gradient ($p < .001$, $Q_M = 101.44$; Figure 5b). Richness increased with fertilizer treatments where ambient N deposition was low (<6 kg ha^{-1} $year^{-1}$) and declined where ambient N deposition was highest (>10 kg ha^{-1} $year^{-1}$). Relative abundances of ECM were similar in control and fertilized plots ($p = .12$, $Q_M = 2.43$) and the response to fertilization was not correlated with ambient N deposition across the gradient ($p = .65$, $Q_M = 0.21$). Likewise, saprotrophic taxa had similar relative abundances in control and fertilized plots ($p = .16$, $Q_M = 1.94$) and the response to fertilization was not correlated with ambient N deposition ($p = .55$, $Q_M = 0.35$; Figure 2a).

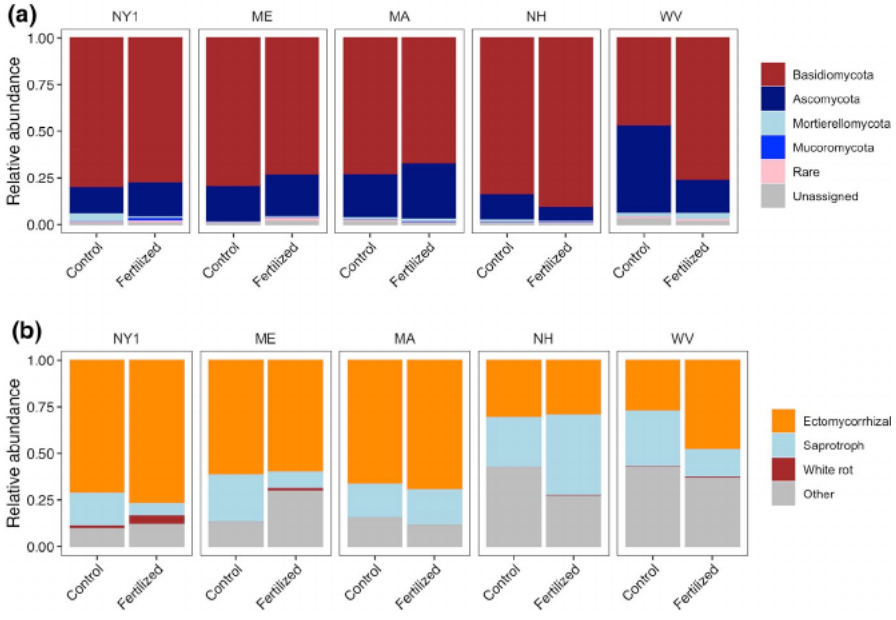

FIGURE 2 Relative abundance of soil fungi representing different phyla (a) and ecologies (b) between control and simulated N deposition (fertilized) treatments (fertilized) (site abbreviations defined in Table 1). Sites are ordered from lowest to highest ambient N deposition (left to right)

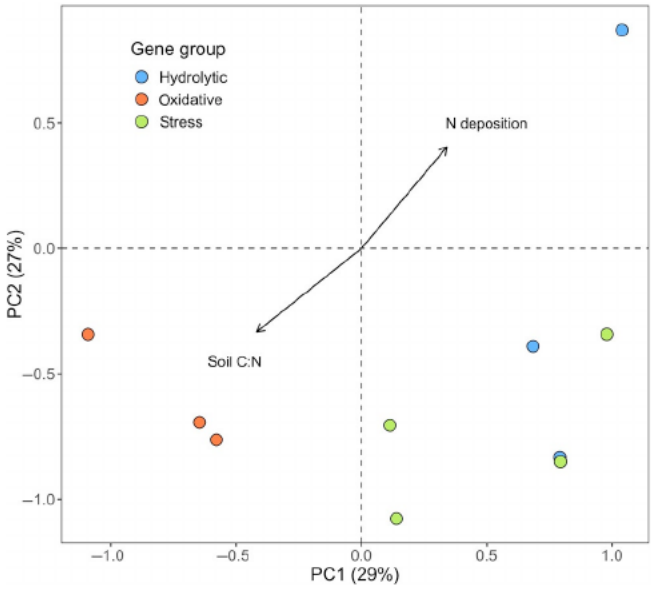

FIGURE 3 Gene variant composition and their relationships with ambient N deposition and soil C:N. Each point represents a gene (e.g., lipH) or gene family (e.g., multicopper oxidases), and colors represent broadly defined gene groups: hydrolytic enzymes, oxidative enzymes, and stress-tolerant genes. For each point, the position was calculated based on relative abundance of that gene across all ambient or control plots at all sites. Points closer together indicate genes with more similar composition of gene variants

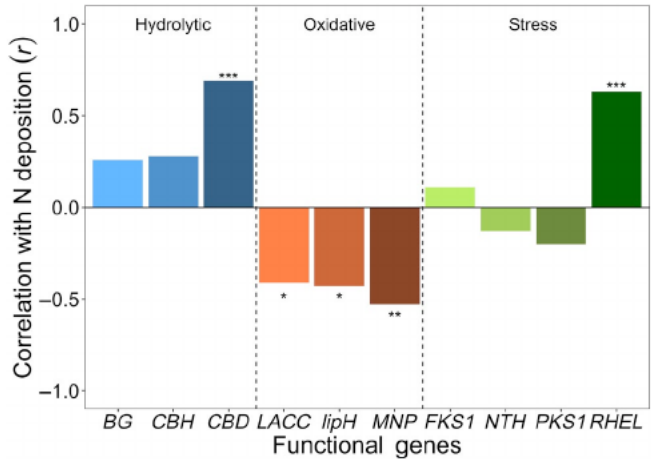

FIGURE 4 Pearson's correlation coefficients of linear relationships between relative abundance of each functional gene and ambient N deposition rate. Functional genes are shown in groups of hydrolytic enzyme-coding genes (*BG*, beta-glucosidase; *CBH*, cellobiohydrolase; *CBD*, cellobioside dehydrogenase), oxidative enzyme-coding genes (*LACC*, laccase; *lipH*, lignin peroxidase; *MNP*, manganese peroxidase), and stress tolerance genes (*FKS1*, beta-1,3-glucan synthase; *NTH*, neutral trehalase; *PKS1*, polyketide synthase; *RHEL*, RNA helicase). Significance is indicated by asterisks (*$p < .05$; **$p < .01$; ***$p < .001$)

Relative abundances of white rot fungi quadrupled with fertilizer treatments ($p = .004$, $Q_M = 8.31$; Figure 2a) from 0.3% in control plots to 1.3% in fertilized plots. However, white rot fungi were only

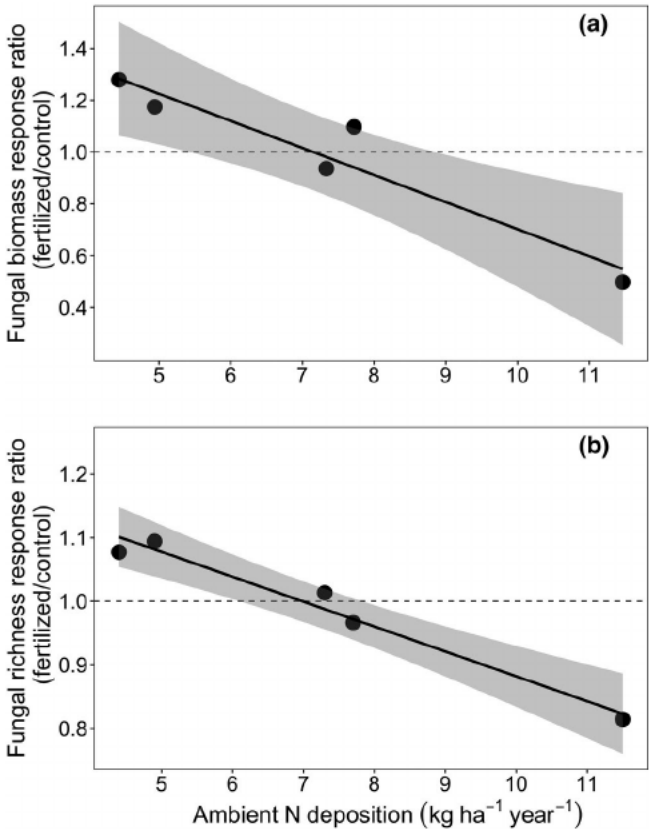

FIGURE 5 Response of fungal biomass (a) and fungal operational taxonomic unit (OTU) richness (b) to N fertilization across the ambient N deposition gradient. Each point represents the ratio of fungal biomass or OTU richness in fertilized relative to control plots at five experimental sites (from lowest to highest ambient N deposition: NY1, ME, MA, NH, and WV). Shaded areas around the trend line represent the 95% CI

detected at three of the five sites with simulated N deposition. The increased relative abundance in white rot fungi was a similar magnitude at each of the three sites they were detected at across the gradient ($p = .34$, $Q_M = 0.89$).

Responses in the relative abundances of different functional gene groups to fertilizer treatments depended on ambient N deposition ($p = .03$, $F = 4.91$; Figure 6; Figure S3). The relative abundance of oxidative enzyme encoding genes decreased with fertilizer treatments, and the effect size increased with ambient N deposition ($p = .02$, $R^2 = .84$; Figure 6a) and pH and decreased with elevation (Table S2). Genes encoding hydrolytic enzymes tended to increase in relative abundance with fertilizer treatments (Figure S3), but the response did not vary with ambient N deposition ($p > .05$; Figure 6b). Functional genes shifted abundance, but gene variant composition did not change with fertilizer treatments across the N deposition gradient. There was no effect of fertilizer treatments on the relative abundance of genes encoding for stress tolerance ($p > .05$; Figure 6c; Figure S3). There was no significant interaction between fertilizer treatments and ambient N deposition on the composition of functional genes ($p = .36$, $F = 1.03$; Figure S3).

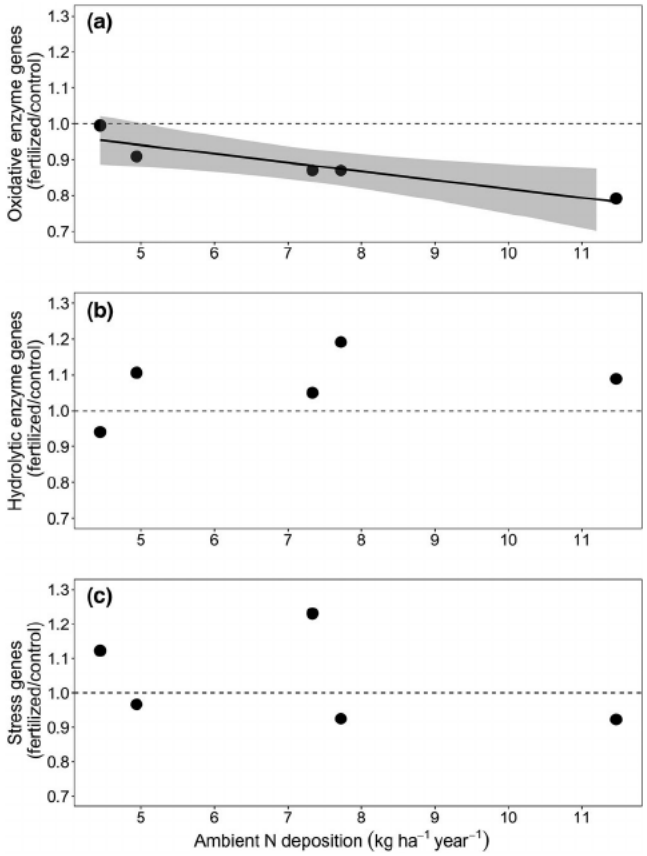

FIGURE 6 Relative abundance of genes coding for oxidative enzymes (a), hydrolytic enzymes (b), or stress tolerance traits (c) at sites varying in ambient N deposition. Points represent the response ratio at individual sites. The horizontal gray dashed line indicates an equal response in N addition relative to control plots. Shaded areas represent the 95% CI around the trendline

4 | DISCUSSION

This is the first study to document fungal community responses in combination with fungal functional potential across a network of fertilizer experiments spanning an ambient N deposition gradient at a large spatial scale. We found that soil fungal community and functional potential responses to fertilizer treatments depended on ambient N deposition which may explain why belowground responses to N additions often vary in magnitude (Yue et al., 2017). Although total fungal biomass did not vary with ambient or simulated N deposition, community composition was highly dissimilar across the N deposition gradient and that community dissimilarity could not be explained by latitude (Table 3). We found that unique ECM fungi were indicators of community composition in forests with low ambient N deposition while unique saprotrophic fungi were indicative of forests experiencing higher ambient N deposition levels. This result may reflect the long-term selective pressure of additional N. Notably, the fungal community associated with high ambient N deposition was negatively correlated with relative abundances of decomposition-related genes and positively correlated with stress response genes. At low levels of ambient N deposition, the community composition may be driven by selection for taxa that can depolymerize organic matter to obtain inorganic N. At high levels of ambient deposition, selection pressures may include increased eutrophication and acidity (Gilliam et al., 1994) as well as limitation of micronutrients (Whalen et al., 2018). Thus, fungal communities were compositionally and functionally distinct across the ambient N deposition gradient, and the effect of N fertilization on fungal communities was predictable based on background N deposition levels. Notably, fungal biomass and taxonomic richness were reduced by fertilizer treatments in forests with high ambient N deposition while they increased in forests with low ambient N deposition. Additionally, oxidative enzyme encoding genes were reduced by increasing ambient N deposition, whereas hydrolytic enzyme encoding genes increased. Fungal genes encoding proteins involved in stress tolerance had different associations with N deposition, potentially because the stress-response proteins we selected are not specific enough to N-induced stress. One of the four stress-response genes we selected, RHEL, indicates a general physiological response to environmental stress and it increased relative abundance with ambient N deposition rate (Figure 4). When taken together, our results suggest that divergent fungal responses to fertilizer addition across the ambient N gradient may be due to alleviation of fungal N limitation where ambient N deposition is low and induced physiological stress where it is high.

Fungal community composition was highly dissimilar across the ambient N deposition gradient and was associated with N mineralization and the abundance of decomposition and stress tolerance genes. Fungal communities have been documented previously to respond to chronic N addition with increased abundance of taxa with low decomposition potential (Morrison et al., 2016, 2018; Whalen et al., 2018). While we detected that fertilizer treatments slightly increased white rot fungal relative abundance, a guild of fungi presumed capable of completely decomposing lignified organic matter, the opposite pattern was observed for the relative abundance of actual oxidative enzyme encoding genes. Together, these results highlight the importance of investigating functional genes in addition to taxonomic shifts since relative abundances of fungal guilds does not always align with actual functional potential. Changes in decomposition potential with N deposition were similar to previous findings (Morrison et al., 2016) and may be related to reduced abundance of oxidative enzyme encoding genes, such as laccase (e.g., observed in this study and Hofmockel et al., 2007), or downregulation of these genes. However, decomposition rates may further depend on whether fungal communities are selected for stress tolerance. Microbial communities are hypothesized to tradeoff decomposition potential for stress response (Lustenhouwer et al., 2020; Treseder & Lennon, 2015), and our results suggest that high ambient N deposition favors stress tolerance over decomposition. We measured total soil organic C in this study, but we hypothesize that particulate organic carbon may be less decomposed due to the selection of stress tolerant fungal taxa with weak decomposing abilities, whereas mineral-associated organic carbon may be

reduced because stress tolerance can reduce microbial growth efficiency (Malik et al., 2020). Selection for stress tolerant fungi is a new lens for understanding why soil organic C tends to accumulate in temperate forests subjected to long-term N addition (Averill & Waring, 2018; Frey et al., 2014).

Nitrogen deposition is known to affect fungal community composition, even with large heterogeneity across complex environmental gradients (Cox et al., 2010). We found that ECM were indicators of community composition where ambient N deposition was low and saprotrophic fungi were the primary indicators where N deposition was high. Half of the indicator species across the ambient N deposition gradient were ECM, which lends support to the idea that ECM are particularly sensitive to N deposition (Lilleskov et al., 2019; Treseder et al., 2005; Table 4). ECM with morphological plasticity, and thus the ability to modulate exploration strategies under different conditions, respond positively to N deposition and other environmental stressors (Morrison et al., 2016). Many ECM taxa are endemic at regional spatial scales (Talbot et al., 2014) and our results suggest that ECM taxa at low N deposition sites may be particularly sensitive to N deposition, whereas a suite of saprotrophic fungi may be selected for under high N deposition. Changes in ECM and saprotrophic fungal membership can have major implications for local beta-diversity with the loss of ECM taxa but gain in saprotrophic fungal taxa fundamentally altering community composition.

Fungal biomass and OTU richness increased with N fertilizer additions where ambient N deposition was low and decreased with fertilizer where ambient N deposition was high. In forests with low ambient N deposition, we presume fungal growth and activity was limited by N availability and that experimental N addition alleviated this limitation. Decomposition rates are positively correlated with N availability in other long-term experiments where background N deposition was comparable to the low ambient N deposition sites in our study gradient (Hu et al., 2001; Neff et al., 2002; Pregitzer et al., 2008). Enrichment of N in forests with low background N deposition could select for taxa that otherwise cannot tolerate low N availability, explaining our observed increase in fungal richness. On the other hand, sites with high ambient deposition fungal biomass and richness were reduced by N addition. We hypothesize that fungal biomass and richness were reduced at sites with high ambient N deposition due to physiological stress crossing a threshold following fertilizer treatments. Inorganic nitrogen can acidify soils, and indeed, we found soil pH was more acidic at high compared to low ambient N deposition sites. Soil acidification caused by N deposition is largely hypothesized to reduce microbial growth and in turn microbial biomass (Averill & Waring, 2018). In addition to soil acidification, limitation of micronutrients induced by N deposition may cause physiological stress in fungi. For example, N addition can exacerbate limitation of manganese (van Diepen et al., 2015), which is critical for production of fungal extracellular enzymes, particularly those related to lignin degradation (Whalen et al., 2018). Our results suggest that lower fungal biomass observed at sites with high soil N loading may result in slowed decomposition as fungi are pushed beyond a stress threshold.

Functional genes conferring decomposition traits responded differentially to ambient N deposition. Oxidative enzyme encoding genes decreased while hydrolytic enzyme encoding genes increased with ambient N deposition. Oxidative enzyme encoding gene composition was more constrained than hydrolytic encoding or stress tolerance encoding gene compositions. Half of the fungal functional gene abundances we investigated were significantly correlated with ambient N deposition. The strongest correlations were between ambient N deposition and CBD (hydrolytic enzyme), MNP (oxidative enzyme), and RNA helicase (stress tolerance protein). Oxidative enzyme activity has been previously shown to decline with N deposition (Chen et al., 2018; Jian et al., 2016), and our study corroborates this previous work showing that the genetic potential for oxidative enzyme production is reduced by high N deposition. We demonstrate a genetic link from shifts in oxidative versus hydrolytic gene abundances that is related to changes in enzyme activity induced by N addition experiments that had ramifications for ecosystem soil C storage (Chen et al., 2018). We emphasize that our study demonstrates *genetic potential* for enzymatic functions; shifts in gene composition are not always correlated with shifts in measurable functions (Zak et al., 2019). The reduction in oxidative enzyme encoding genes with ambient N deposition may be related to declines in fungal taxa that oxidize organic matter and possibly the accumulation of organic matter with N fertilization (Carreiro et al., 2000).

White rot fungi are a polyphyletic group largely associated with lignin decomposition (Floudas et al., 2012). While lignin decomposition declines with N addition, our study and others have found that white rot fungi have increased relative abundance with N addition (Entwistle et al., 2017); yet; the increased abundance is not correlated with ligninase activity (Morrison et al., 2016). This incongruence between white rot fungal abundance and ligninase activity warrants further investigation. For example, transcriptomic or proteomic characterization of fungal activity could explain what enzymes these white rot fungi are deploying in addition to oxidative enzymes because they are also capable of decomposing more labile forms of soil organic matter (Floudas et al., 2012). Basidiomycete laccase genes have been documented previously to decline with N deposition in forests where leaf litter contains more lignin (black oak/white oak) relative to forests with low foliar lignin content (sugar maple-basswood; Hofmockel et al., 2007). Suppression of lignin-modifying enzymes due to N deposition results in accumulation of soil C stocks as decomposition is impeded (Chen et al., 2018).

Although the composition of stress tolerance gene variants shifted in associating with fungal community composition characteristic of high N deposition, the total relative abundance of protein-encoding genes related to stress tolerance did not directly correlate with N deposition. One stress tolerance gene, RHEL, was correlated with ambient N deposition. RNA helicase is important in cold tolerance as it prevents formation of structures on RNA that would impact translation. RNA helicases may be part of a generalized abiotic stress response system that rearranges RNA secondary structure to influence biochemical cascades (Owttrim, 2013). This remains an active research topic and much is still unknown about how fungi tolerate

abiotic stress. Suites of traits enabling stress tolerance in fungi may respond to N deposition, but it is possible that we targeted stress tolerance traits that were overly general to explain the full catalogue of stress response genes conferring resistance to N deposition. Little is known about fungal stress tolerance (Treseder & Lennon, 2015) and few fungal stress genes exist in databases needed to develop probes for target-gene enrichment. Genes we recommend targeting in future studies are specific to how fungi respond to N deposition stress. Stress induced by N deposition could be related to soil acidification, and thus genes encoding proton pumps may become more abundant (e.g., glutamate decarboxylase). Nitrogen deposition also changes micronutrient availability (van Diepen et al., 2015) which, in turn, affects fungal decay capacity and community composition (Whalen et al., 2018). Genes that are specific for enzymes used to acquire micronutrients could elucidate whether micronutrient limitation is related to shifts in fungal communities and functions with ambient N deposition. While much work has been done on fungal decomposition responses to N deposition, stress responses remain relatively unexplored. We hypothesize that the combination of reduced decomposition and increased stress tolerance capacity observed in association with particular fungal communities synergistically mediates ecosystem C stock responses to N deposition.

In conclusion, our study revealed that soil biogeochemical and fungal responses to N additions depend on background ambient N deposition levels. Fungal biomass and richness increased with fertilizer treatments at sites with low (<6 kg ha^{-1} $year^{-1}$) and decreased at sites with high (>8 kg ha^{-1} $year^{-1}$) ambient N deposition. Different fungal communities were found across the gradient of ambient N deposition with ECM being indicator taxa at low ambient N deposition and saprotrophs being indicators at high ambient N deposition sites. Oxidative enzyme encoding genes declined and hydrolytic enzyme encoding genes increased with ambient N deposition. We did not find evidence for increased stress tolerance encoding gene relative abundance which warrants further attention targeting specific stress response systems more relevant to N addition induced stress. Whether there is a tradeoff in fungal decomposition versus stress tolerance encoding genes with fertilizer treatments or ambient N deposition remains an open question.

ACKNOWLEDGEMENTS

We thank Mel Knorr, Christine Bunyon, Christina Lyons, and Leana Axtell for assistance with sample collection and laboratory analyses. We also thank the following site managers and personnel for access to sites and archived data: Bill Schuster (Black Rock Forest Consortium), Frank Gilliam and Bill Peterjohn (Fernow Experimental Forest), Susan Stout (Kane Experimental Forest), Gary Lovett (Cary Institute of Ecosystem Studies), Melany Fisk (Bartlett Experimental Forest), and Ivan Fernandez (Bear Brook Watershed). We acknowledge the TDep Science Committee of the National Atmospheric Deposition Program (NADP) for making data publicly available. J.A.M.M. was partially supported by Postdoctoral Development funding from Oak Ridge National Laboratory. The Chronic Nitrogen Addition Study at the Harvard Forest Long-term Ecological Research (LTER) site is supported through the NSF LTER Program (DEB-1832110). L.K.T. was supported by grant no. UMO-2017/26/E/NZ8/00057 (National Science Centre, Poland). We declare no conflicts of interest.

DATA AVAILABILITY STATEMENT

Sequences obtained in this study have been archived with the US National Center for Biotechnology Information (NCBI; https://www.ncbi.nlm.nih.gov) under BioProject accession number PRJNA672870. Environmental data have been archived with the US Environmental Data Initiative (https://doi.org/10.6073/pasta/c67bff6613b12a96e0d78de3727b0178).

ORCID

Jessica A. M. Moore https://orcid.org/0000-0002-5387-0662
Artur Trzebny https://orcid.org/0000-0002-0831-7243
Kevin M. Geyer https://orcid.org/0000-0002-5218-2745

REFERENCES

Aber, J. D., Goodale, C. L., Ollinger, S. V., Smith, M.-L., Magill, A. H., Martin, M. E., Hallett, R. A., & Stoddard, J. L. (2003). Is nitrogen deposition altering the nitrogen status of northeastern forests? *BioScience*, *53*, 375–389.

Averill, C., & Waring, B. (2018). Nitrogen limitation of decomposition and decay: How can it occur? *Global Change Biology*, *24*, 1417–1427. https://doi.org/10.1111/gcb.13980

Aylward, M. L., Sullivan, A. P., Perry, G. H., Johnson, S. E., & Louis Jr., E. E. (2018). An environmental DNA sampling method for aye-ayes from their feeding traces. *Ecology and Evolution*, *8*, 9229–9240. https://doi.org/10.1002/ece3.4341

Bartoń, K. (2020). *MuMIn: Multi-model inference*. R package version 1.43.17. Retrieved from https://CRAN.R-project.org/package=MuMIn

Benson, D. A., Karsch-Mizrachi, I., Lipman, D. J., Ostell, J., & Wheeler, D. L. (2005). GenBank. *Nucleic Acids Research*, *33*, D34–D38. https://doi.org/10.1093/nar/gki063

Bolger, A. M., Lohse, M., & Usadel, B. (2014). Trimmomatic: A flexible trimmer for Illumina sequence data. *Bioinformatics*, *30*, 2114–2120. https://doi.org/10.1093/bioinformatics/btu170

Bowman, W. D., Cleveland, C. C., Halada, L., Hresko, J., & Baron, J. S. (2008). Negative impact of nitrogen deposition on soil buffering capacity. *Nature Geoscience*, *1*, 767–770. https://doi.org/10.1038/ngeo339

Braman, R. S., & Hendrix, S. A. (1989). Nanogram nitrite and nitrate determination in environmental and biological materials by vanadium (III) reduction with chemiluminescence detection. *Analytical Chemistry*, *61*, 2715–2718. https://doi.org/10.1021/ac00199a007

Burke, D. J., Weintraub, M. N., Hewins, C. R., & Kalisz, S. (2011). Relationship between soil enzyme activities, nutrient cycling and soil fungal communities in a northern hardwood forest. *Soil Biology and Biochemistry*, *43*, 795–803. https://doi.org/10.1016/j.soilbio.2010.12.014

Cairney, J. W. G. (2012). Extramatrical mycelia of ectomycorrhizal fungi as moderators of carbon dynamics in forest soil. *Soil Biology and Biochemistry*, *47*, 198–208. https://doi.org/10.1016/j.soilbio.2011.12.029

Caporaso, J. G., Kuczynski, J., Stombaugh, J., Bittinger, K., Bushman, F. D., Costello, E. K., Fierer, N., Pena, A. G., Goodrich, J. K., & Gordon, J. I. (2010). QIIME allows analysis of high-throughput community sequencing data. *Nature Methods*, *7*, 335.

Carreiro, M., Sinsabaugh, R., Repert, D., & Parkhurst, D. (2000). Microbial enzyme shifts explain litter decay responses to simulated nitrogen deposition. *Ecology*, *81*, 2359–2365.

Chen, J., Luo, Y., Van Groenigen, K. J., Hungate, B. A., Cao, J., Zhou, X., & Wang, R. W. (2018). A keystone microbial enzyme for nitrogen control of soil carbon storage. *Science Advances*, *4*, eaaq1689. https://doi.org/10.1126/sciadv.aaq1689

Contosta, A. R., Frey, S. D., & Cooper, A. B. (2011). Seasonal dynamics of soil respiration and N mineralization in chronically warmed and fertilized soils. *Ecosphere*, *2*, 1–21. https://doi.org/10.1890/es10-00133.1

Cox, F., Barsoum, N., Lilleskov, E. A., & Bidartondo, M. I. (2010). Nitrogen availability is a primary determinant of conifer mycorrhizas across complex environmental gradients. *Ecology Letters*, *13*, 1103–1113. https://doi.org/10.1111/j.1461-0248.2010.01494.x

De Caceres, M., & Legendre, P. (2009). Associations between species and groups of sites: indices and statistical inference. R package version 1.6. Retrived from http://sites.google.com/site/miqueldecaceres/

DeForest, J. L., Zak, D. R., Pregitzer, K. S., & Burton, A. J. (2004). Atmospheric nitrate deposition, microbial community composition, and enzyme activity in northern hardwood forests. *Soil Science Society of America Journal*, *68*, 132–138. https://doi.org/10.2136/sssaj2004.1320

Dowle, E. J., Pochon, X., Banks, J. C., Shearer, K., & Wood, S. A. (2016). Targeted gene enrichment and high-throughput sequencing for environmental biomonitoring: A case study using freshwater macroinvertebrates. *Molecular Ecology Resources*, *16*, 1240–1254. https://doi.org/10.1111/1755-0998.12488

Drosou, K., Price, C., & Brown, T. A. (2018). The kinship of two 12th Dynasty mummies revealed by ancient DNA sequencing. *Journal of Archaeological Science: Reports*, *17*, 793–797. https://doi.org/10.1016/j.jasrep.2017.12.025

Edgar, R. C. (2010). Search and clustering orders of magnitude faster than BLAST. *Bioinformatics*, *26*, 2460–2461. https://doi.org/10.1093/bioinformatics/btq461

Edgar, R. (2016). SINTAX: A simple non-Bayesian taxonomy classifier for 16S and ITS sequences. *BioRxiv*, 074161. https://doi.org/10.1101/074161

Eisenlord, S. D., Freedman, Z., Zak, D. R., Xue, K., He, Z., & Zhou, J. (2013). Microbial mechanisms mediating increased soil C storage under elevated atmospheric N deposition. *Applied and Environmental Microbiology*, *79*, 1191–1199. https://doi.org/10.1128/aem.03156-12

Ekblad, A., Wallander, H., Godbold, D. L., Cruz, C., Johnson, D., Baldrian, P., Björk, R., Epron, D., Kieliszewska-Rokicka, B., & Kjøller, R. (2013). The production and turnover of extramatrical mycelium of ectomycorrhizal fungi in forest soils: Role in carbon cycling. *Plant and Soil*, *366*, 1–27. https://doi.org/10.1007/s11104-013-1630-3

Entwistle, E. M., Zak, D. R., & Argiroff, W. A. (2017). Anthropogenic N deposition increases soil C storage by reducing the relative abundance of lignolytic fungi. *Ecological Monographs*, *88*, 225–244. https://doi.org/10.1002/ecm.1288

Entwistle, E. M., Zak, D. R., & Edwards, I. P. (2013). Long-term experimental nitrogen deposition alters the composition of the active fungal community in the forest floor. *Soil Science Society of America Journal*, *77*, 1648–1658. https://doi.org/10.2136/sssaj2013.05.0179

Erisman, J. W., Galloway, J. N., Seitzinger, S., Bleeker, A., Dise, N. B., Petrescu, A. R., Leach, A. M., & de Vries, W. (2013). Consequences of human modification of the global nitrogen cycle. *Philosophical Transactions of the Royal Society B: Biological Sciences*, *368*, 20130116. https://doi.org/10.1098/rstb.2013.0116

Fierer, N., Leff, J. W., Adams, B. J., Nielsen, U. N., Bates, S. T., Lauber, C. L., Owens, S., Gilbert, J. A., Wall, D. H., & Caporaso, J. G. (2012). Cross-biome metagenomic analyses of soil microbial communities and their functional attributes. *Proceedings of the National Academy of Sciences of the United States of America*, *109*, 21390–21395. https://doi.org/10.1073/pnas.1215210110

Floudas, D., Binder, M., Riley, R., Barry, K., Blanchette, R. A., Henrissat, B., Martinez, A. T., Otillar, R., Spatafora, J. W., Yadav, J. S., Aerts, A., Benoit, I., Boyd, A., Carlson, A., Copeland, A., Coutinho, P. M., de Vries, R. P., Ferreira, P., Findley, K., … Hibbett, D. S. (2012). The Paleozoic origin of enzymatic lignin decomposition reconstructed from 31 fungal genomes. *Science*, *336*, 1715–1719. https://doi.org/10.1126/science.1221748

Freedman, Z. B., Romanowicz, K. J., Upchurch, R. A., & Zak, D. R. (2015). Differential responses of total and active soil microbial communities to long-term experimental N deposition. *Soil Biology and Biochemistry*, *90*, 275–282. https://doi.org/10.1016/j.soilbio.2015.08.014

Frey, S. D., Knorr, M., Parrent, J. L., & Simpson, R. T. (2004). Chronic nitrogen enrichment affects the structure and function of the soil microbial community in temperate hardwood and pine forests. *Forest Ecology and Management*, *196*, 159–171. https://doi.org/10.1016/j.foreco.2004.03.018

Frey, S. D., Ollinger, S., Nadelhoffer, K., Bowden, R., Brzostek, E., Burton, A., Caldwell, B. A., Crow, S., Goodale, C. L., Grandy, A. S., Finzi, A., Kramer, M. G., Lajtha, K., LeMoine, J., Martin, M., McDowell, W. H., Minocha, R., Sadowsky, J. J., Templer, P. H., & Wickings, K. (2014). Chronic nitrogen additions suppress decomposition and sequester soil carbon in temperate forests. *Biogeochemistry*, *121*, 305–316. https://doi.org/10.1007/s10533-014-0004-0

Galloway, J. N., & Cowling, E. B. (2002). Reactive nitrogen and the world: 200 years of change. *Ambio*, *31*, 64–72. https://doi.org/10.1579/0044-7447-31.2.64

Gilliam, F. S., Burns, D. A., Driscoll, C. T., Frey, S. D., Lovett, G. M., & Watmough, S. A. (2019). Decreased atmospheric nitrogen deposition in eastern North America: Predicted responses of forest ecosystems. *Environmental Pollution*, *244*, 560–574. https://doi.org/10.1016/j.envpol.2018.09.135

Gilliam, F. S., Turrill, N. L., Aulick, S. D., Evans, D. K., & Adams, M. B. (1994). Herbaceous layer and soil responses to experimental acidification in a central Appalachian hardwood forest. *Journal of Environmental Quality*, *23*, 835–844. https://doi.org/10.2134/jeq1994.00472425002300040032x

Gilliam, F. S., Welch, N. T., Phillips, A. H., Billmyer, J. H., Peterjohn, W. T., Fowler, Z. K., Walter, C. A., Burnham, M. B., May, J. D., & Adams, M. B. (2016). Twenty-five-year response of the herbaceous layer of a temperate hardwood forest to elevated nitrogen deposition. *Ecosphere*, *7*, e01250. https://doi.org/10.1002/ecs2.1250

Guckert, J. B., Antworth, C. P., & Nichols, P. D. (1985). Phospholipid, ester-linked fatty acid profiles as reproducible assays for changes in prokaryotic community structure of estuarine sediments. *FEMS Microbiology Ecology*, *31*, 147–158. https://doi.org/10.1111/j.1574-6968.1985.tb01143.x

Hannon, G. J. (2010). Fastx-toolkit. Computer program distributed by the author.

Hassett, J. E., Zak, D. R., Blackwood, C. B., & Pregitzer, K. S. (2009). Are basidiomycete laccase gene abundance and composition related to reduced lignolytic activity under elevated atmospheric NO_3^- Deposition in a northern hardwood forest? *Microbial Ecology*, *57*, 728–739. https://doi.org/10.1007/s00248-008-9440-5

Heintzman, P. D., Zazula, G. D., MacPhee, R. D., Scott, E., Cahill, J. A., McHorse, B. K., Kapp, J. D., Stiller, M., Wooller, M. J., & Orlando, L. (2017). A new genus of horse from Pleistocene North America. *Elife*, *6*, e29944. https://doi.org/10.7554/elife.29944

Hendricks, S. A., Schweizer, R. M., Harrigan, R. J., Pollinger, J. P., Paquet, P. C., Darimont, C. T., Adams, J. R., Waits, L. P., vonHoldt, B. M., Hohenlohe, P. A., & Wayne, R. K. (2019). Natural re-colonization and admixture of wolves (*Canis lupus*) in the US Pacific Northwest: Challenges for the protection and management of rare and endangered taxa. *Heredity*, *122*, 133–149. https://doi.org/10.1038/s41437-018-0094-x

Hesse, C. N., Mueller, R. C., Vuyisich, M., Gallegos-Graves, L. V., Gleasner, C. D., Zak, D. R., & Kuske, C. R. (2015). Forest floor community

metatranscriptomes identify fungal and bacterial responses to N deposition in two maple forests. *Frontiers in Microbiology*, *6*, 337. https://doi.org/10.3389/fmicb.2015.00337

Hofmockel, K. S., Zak, D. R., & Blackwood, C. B. (2007). Does atmospheric NO_3^- – Deposition alter the abundance and activity of lignin-olytic fungi in forest soils? *Ecosystems*, *10*, 1278–1286. https://doi.org/10.1007/s10021-007-9096-x

Högberg, M. N., & Högberg, P. (2002). Extramatrical ectomycorrhizal mycelium contributes one-third of microbial biomass and produces, together with associated roots, half the dissolved organic carbon in a forest soil. *New Phytologist*, *154*, 791–795. https://doi.org/10.1046/j.1469-8137.2002.00417.x

Hu, S., Chapin, F. S., Firestone, M. K., Field, C. B., & Chiariello, N. R. (2001). Nitrogen limitation of microbial decomposition in a grassland under elevated CO_2. *Nature*, *409*, 188–191. https://doi.org/10.1038/35051576

Jian, S., Li, J., Chen, J., Wang, G., Mayes, M. A., Dzantor, K. E., Hui, D., & Lou, Y. (2016). Soil extracellular enzyme activities, soil carbon and nitrogen storage under nitrogen fertilization: A meta-analysis. *Soil Biology and Biochemistry*, *101*, 32–43. https://doi.org/10.1016/j.soilbio.2016.07.003

Kang, H., Fahey, T. J., Bae, K., Fisk, M., Sherman, R. E., Yanai, R. D., & See, C. R. (2016). Response of forest soil respiration to nutrient addition depends on site fertility. *Biogeochemistry*, *127*, 113–124. https://doi.org/10.1007/s10533-015-0172-6

Kircher, M., Sawyer, S., & Meyer, M. (2012). Double indexing overcomes inaccuracies in multiplex sequencing on the Illumina platform. *Nucleic Acids Research*, *40*, (1), e3. https://doi.org/10.1093/nar/gkr771

Knorr, M., Frey, S., & Curtis, P. (2005). Nitrogen additions and litter decomposition: A meta-analysis. *Ecology*, *86*, 3252–3257. https://doi.org/10.1890/05-0150

Li, H., & Durbin, R. (2010). Fast and accurate long-read alignment with Burrows-Wheeler transform. *Bioinformatics*, *26*, 589–595. https://doi.org/10.1093/bioinformatics/btp698

Lilleskov, E. A., Bruns, T. D., Horton, T. R., Lee Taylor, D., & Grogan, P. (2004). Detection of forest stand-level spatial structure in ectomycorrhizal fungal communities. *FEMS Microbiology Ecology*, *49*, 319–332. https://doi.org/10.1016/j.femsec.2004.04.004

Lilleskov, E. A., Kuyper, T. W., Bidartondo, M. I., & Hobbie, E. A. (2019). Atmospheric nitrogen deposition impacts on the structure and function of forest mycorrhizal communities: A review. *Environmental Pollution*, *246*, 148–162. https://doi.org/10.1016/j.envpol.2018.11.074

Liu, L., & Greaver, T. L. (2010). A global perspective on belowground carbon dynamics under nitrogen enrichment. *Ecology Letters*, *13*, 819–828. https://doi.org/10.1111/j.1461-0248.2010.01482.x

Loreille, O., Ratnayake, S., Bazinet, A., Stockwell, T., Sommer, D., Rohland, N., Mallick, S., Johnson, P., Skoglund, P., Onorato, A., Bergman, N., Reich, D., & Irwin, J. (2018). Biological sexing of a 4000-year-old Egyptian mummy head to assess the potential of nuclear DNA recovery from the most damaged and limited forensic specimens. *Genes*, *9*, 135. https://doi.org/10.3390/genes9030135

Lovett, G. M., Arthur, M. A., Weathers, K. C., Fitzhugh, R. D., & Templer, P. H. (2013). Nitrogen addition increases carbon storage in soils, but not in trees, in an eastern US deciduous forest. *Ecosystems*, *16*, 980–1001. https://doi.org/10.1007/s10021-013-9662-3

Lovett, G. M., & Goodale, C. L. J. E. (2011). A new conceptual model of nitrogen saturation based on experimental nitrogen addition to an oak forest. *Frontiers in Ecology and Evolution*, *14*, 615–631. https://doi.org/10.1007/s10021-011-9432-z

Lovett, G. M., Goodale, C. L., Ollinger, S. V., Fuss, C. B., Ouimette, A. P., & Likens, G. E. (2018). Nutrient retention during ecosystem succession: A revised conceptual model. *Frontiers in Ecology and the Environment*, *16*(9), 532–538. https://doi.org/10.1002/fee.1949

Lustenhouwer, N., Maynard, D. S., Bradford, M. A., Lindner, D. L., Oberle, B., Zanne, A. E., & Crowther, T. W. (2020). A trait-based understanding of wood decomposition by fungi. *Proceedings of the National Academy of Sciences of the United States of America*, *117*, 11551–11558. https://doi.org/10.1073/pnas.1909166117

Magill, A. H., & Aber, J. D. (1998). Long-term effects of experimental nitrogen additions on foliar litter decay and humus formation in forest ecosystems. *Plant and Soil*, *203*, 301–311. https://doi.org/10.1023/a:1004367000041

Malik, A. A., Martiny, J. B. H., Brodie, E. L., Martiny, A. C., Treseder, K. K., & Allison, S. D. (2020). Defining trait-based microbial strategies with consequences for soil carbon cycling under climate change. *The ISME Journal*, *14*, 1–9. https://doi.org/10.1038/s41396-019-0510-0

Minocha, R., Long, S., Turlapati, S. A., & Fernandez, I. J. (2019). Dynamic species-specific metabolic changes in the trees exposed to chronic N+S additions at the Bear Brook Watershed in Maine, USA. *Annals of Forest Science*, *76*(1). https://doi.org/10.1007/s13595-019-0808-0

Morrison, E. W., Frey, S. D., Sadowsky, J. J., van Diepen, L. T., Thomas, W. K., & Pringle, A. (2016). Chronic nitrogen additions fundamentally restructure the soil fungal community in a temperate forest. *Fungal Ecology*, *23*, 48–57. https://doi.org/10.1016/j.funeco.2016.05.011

Morrison, E. W., Pringle, A., van Diepen, L. T., & Frey, S. D. (2018). Simulated nitrogen deposition favors stress-tolerant fungi with low potential for decomposition. *Soil Biology and Biochemistry*, *125*, 75–85. https://doi.org/10.1016/j.soilbio.2018.06.027

National Atmospheric Deposition Program. (2016). *NADP data report 2016-02*. University of Illinois at Urbana-Champaign.

Nave, L., Vance, E., Swanston, C., & Curtis, P. (2009). Impacts of elevated N inputs on north temperate forest soil C storage, C/N, and net N-mineralization. *Geoderma*, *153*, 231–240. https://doi.org/10.1016/j.geoderma.2009.08.012

Neff, J. C., Townsend, A. R., Gleixner, G., Lehman, S. J., Turnbull, J., & Bowman, W. D. (2002). Variable effects of nitrogen additions on the stability and turnover of soil carbon. *Nature*, *419*, 915–917. https://doi.org/10.1038/nature01136

Nguyen, N. H., Song, Z., Bates, S. T., Branco, S., Tedersoo, L., Menke, J., Schilling, J. S., & Kennedy, P. G. (2016). FUNGuild: An open annotation tool for parsing fungal community datasets by ecological guild. *Fungal Ecology*, *20*, 241–248. https://doi.org/10.1016/j.funeco.2015.06.006

Norton S., Kahl J., Fernandez I., Haines T., Rustad L., Nodvin S., Scofield J., Strickland T., Erickson H., Wigington Jr. P., & Lee J. (1999). *Environmental Monitoring and Assessment*, *55*, (1), 7–51. https://doi.org/10.1023/a:1006115011381

Oksanen, J., Blanchet, F. G., Kindt, R., Legendre, P., Minchin, P. R., O'hara, R., Simpson, G. L., Solymos, P., Stevens, M. H. H., & Wagner, H. (2013). Package 'vegan'. Community ecology package, version 2, 1–295.

Owttrim G. W. (2013). RNA helicases. *RNA Biology*, *10*, (1), 96–110. https://doi.org/10.4161/rna.22638

Pregitzer, K. S., Burton, A. J., Zak, D. R., & Talhelm, A. F. (2008). Simulated chronic nitrogen deposition increases carbon storage in Northern Temperate forests. *Global Change Biology*, *14*, 142–153. https://doi.org/10.1111/j.1365-2486.2007.01465.x

Rabinovich, M., Bolobova, A., & Vasil'Chenko, L. G. (2004). Fungal decomposition of natural aromatic structures and xenobiotics: A review. *Applied Biochemistry Microbiology*, *40*, 1–17. https://doi.org/10.1023/B:ABIM.0000010343.73266.08

Robertson, G. P., Coleman, D. C., Bledsoe, C. S., & Sollins, P. (1999). *Standard soil methods for long-term ecological research*. Oxford University Press.

Saiya-Cork, K. R., Sinsabaugh, R. L., & Zak, D. R. (2002). The effects of long term nitrogen deposition on extracellular enzyme activity in an *Acer saccharum* forest soil. *Soil Biology & Biochemistry*, *34*, 1309–1315. https://doi.org/10.1016/S0038-0717(02)00074-3

Sinsabaugh, R. L., Carreiro, M. M., & Alvarez, S. (2002). Enzyme and microbial dynamics of litter decomposition. In M. Dekker (Ed.), *Enzymes*

in the environment, activity, ecology applications (pp. 249–265). Boca Raton, FL: CRC Press.

Talbot, J. M., Bruns, T. D., Taylor, J. W., Smith, D. P., Branco, S., Glassman, S. I., Erlandson, S., Vilgalys, R., Liao, H.-L., & Smith, M. E. (2014). Endemism and functional convergence across the North American soil mycobiome. *Proceedings of the National Academy of Sciences of the United States of America*, *111*, 6341–6346. https://doi.org/10.1073/pnas.1402584111

Treseder, K. K., Allen, M. F., Ruess, R. W., Pregitzer, K. S., & Hendrick, R. L. (2005). Lifespans of fungal rhizomorphs under nitrogen fertilization in a pinyon-juniper woodland. *Plant and Soil*, *270*, 249–255. https://doi.org/10.1007/s11104-004-1559-7

Treseder, K. K., & Lennon, J. T. (2015). Fungal traits that drive ecosystem dynamics on land. *Microbiology and Molecular Biology Reviews*, *79*, 243–262. https://doi.org/10.1128/mmbr.00001-15

van Diepen, L. T. A., Frey, S. D., Landis, E. A., Morrison, E. W., & Pringle, A. (2017). Fungi exposed to chronic nitrogen enrichment are less able to decay leaf litter. *Ecology*, *98*, 5–11. https://doi.org/10.1002/ecy.1635

van Diepen, L. T. A., Frey, S. D., Sthultz, C. M., Morrison, E. W., Minocha, R., & Pringle, A. (2015). Changes in litter quality caused by simulated nitrogen deposition reinforce the N-induced suppression of litter decay. *Ecosphere*, *6*, 205. https://doi.org/10.1890/es15-00262.1

Vance, E., Brookes, P., & Jenkinson, D. (1987). An extraction method for measuring soil microbial biomass C. *Soil Biology and Biochemistry*, *19*, 703–707. https://doi.org/10.1016/0038-0717(87)90052-6

Viechtbauer, W. (2005). Bias and efficiency of meta-analytic variance estimators in the random-effects model. *Journal of Educational and Behavioral Statistics*, *30*, 261–293. https://doi.org/10.3102/10769986030003261

Viechtbauer, W. (2010). Conducting meta-analyses in R with the metafor package. *Journal of Statistical Software*, *36*, 1–48.

Waldrop, M. P., Zak, D. R., Sinsabaugh, R. L., Gallo, M., & Lauber, C. (2004). Nitrogen deposition modifies soil carbon storage through changes in microbial enzymatic activity. *Ecological Applications*, *14*, 1172–1177. https://doi.org/10.1890/03-5120

Wallenstein, M. D., McNulty, S., Fernandez, I. J., Boggs, J., & Schlesinger, W. H. (2006). Nitrogen fertilization decreases forest soil fungal and bacterial biomass in three long-term experiments. *Forest Ecology and Management*, *222*, 459–468. https://doi.org/10.1016/j.foreco.2005.11.002

Whalen, E. D., Smith, R. G., Grandy, A. S., & Frey, S. D. (2018). Manganese limitation as a mechanism for reduced decomposition in soils under atmospheric nitrogen deposition. *Soil Biology and Biochemistry*, *127*, 252–263. https://doi.org/10.1016/j.soilbio.2018.09.025

White, D. C., Davis, W. M., Nickels, J. S., King, J. S., & Bobbie, R. J. (1979). Determination of the sedimentary microbial biomass by extractable lipid phosphate. *Oecologia*, *40*, 51–62. https://doi.org/10.1007/bf00388810

White, T. J., Bruns, T., Lee, S., & Taylor, J. W. (1990). Amplification and direct sequencing of fungal ribosomal RNA genes for phylogenetics. In M. A. Innis, D. H. Gelfand, J. J. Sninsky, & T. J. White (Eds.), *PCR protocols: A guide to methods and applications* (pp. 315–322). Academic Press Inc.

Worrall, J. J., Anagnost, S. E., & Zabel, R. A. (1997). Comparison of wood decay among diverse lignicolous fungi. *Mycologia*, *89*, 199–219. https://doi.org/10.1080/00275514.1997.12026772

Yue, K., Fornara, D. A., Yang, W., Peng, Y., Peng, C., Liu, Z., & Wu, F. (2017). Influence of multiple global change drivers on terrestrial carbon storage: Additive effects are common. *Ecology Letters*, *20*, 663–672. https://doi.org/10.1111/ele.12767

Zak, D. R., Argiroff, W. A., Freedman, Z. B., Upchurch, R. A., Entwistle, E. M., & Romanowicz, K. J. (2019). Anthropogenic N deposition, fungal gene expression, and an increasing carbon sink in the Northern Hemisphere. *Ecology*, *100*, e02804. https://doi.org/10.1002/ecy.2804

Zak, D. R., Pregitzer, K. S., Burton, A. J., Edwards, I. P., & Kellner, H. (2011). Microbial responses to a changing environment: Implications for the future functioning of terrestrial ecosystems. *Fungal Ecology*, *4*, 386–395. https://doi.org/10.1016/j.funeco.2011.04.001

Zhang, H., Wang, R., Chen, S., Qi, G., He, Z., & Zhao, X. (2017). Microbial taxa and functional genes shift in degraded soil with bacterial wilt. *Scientific Reports*, *7*, 39911. https://doi.org/10.1038/srep39911

Zhang, T., Chen, H. Y., & Ruan, H. (2018). Global negative effects of nitrogen deposition on soil microbes. *The ISME Journal*, *12*, 1817–1825. https://doi.org/10.1038/s41396-018-0096-y

SUPPORTING INFORMATION

Additional supporting information may be found online in the Supporting Information section.

How to cite this article: Moore JAM, Anthony MA, Pec GJ, et al. Fungal community structure and function shifts with atmospheric nitrogen deposition. *Glob Change Biol*. 2021;27:1349–1364. https://doi.org/10.1111/gcb.15444